Forearm range of motion in *Allosaurus fragilis* (Dinosauria: Theropoda)

Qingqing Liang [a, b], Peter Lewis Falkingham [c], Lida Xing [a, b *]

[a] Frontiers Science Center for Deep-time Digital Earth, China University of Geosciences (Beijing), Beijing 100083, China;

[b] School of the Earth Sciences and Resources, China University of Geosciences (Beijing), Beijing 100083, China

[c] School of Biological and Environmental Sciences, Liverpool John Moores University, Liverpool, UK.

Abstract

Forelimb bones of the Early Jurassic theropod *Allosaurus fragilis* were digitally manipulated based on three-dimensional (3D) digital models. Bony articular surface margins were used as limits to determine the range of motion (ROM) for each forelimb joint, and to test functional hypotheses of forelimb usage. We discuss the effects of palaeopathology at the right shoulder joint on inferring ROM in the forelimb of *Allosaurus*. It is considered that the glenoid aberration of this sub-adult specimen occurred in early ontogeny and lasted for a long period of time, affecting to varying degrees the development of the whole right arm (but not the manus). The relatively large ranges of extension and flexion of manual joints indicate wellgrasping ability consistent with early-diverging theropods. The limited ROM of the shoulder joints of *Allosaurus* suggests that the forelimbs were predominantly prey-acquiring but could go no further forward, indicating that the first contact with prey was made by the mouth. The manus could assist in grasping prey on the chest or below the neck or hooking objects.

Keywords: *Allosaurus*, digital models, forelimbs, range of motion, locomotion, prey

1 Introduction

Palaeobiomechanics is the quantitative study of the mechanical aspects of extinct biological systems. In recent years, vertebrate palaeobiomechanics has gained widespread attention and has provided new insights into the structure, function and motion of ancient animals (like dinosaurs), from whole organisms down to the organs (e.g. Galton 1971; Carpenter 2002; Senter and Parrish 2005; White et al. 2015; Senter and Sullivan 2019; Yu et al. 2022). *Allosaurus fragilis*, named type species by Marsh (1877), is the most common genus of theropod dinosaur in North America in the Late Jurassic Morrison Formation (Late Kimmeridgian-Early Tithonian), known for its remarkable remains of at least 60 individuals (Gilmore 1920; Smith 1998; Chure and Loewen 2020). Investigations of the range of motion (ROM) of parts of *Allosaurus* represent the most commonly reported in palaeobiomechanics (Carpenter 2002; Rayfield 2005; Senter and Parrish 2005; Bates et al. 2012; Snively et al. 2013). Here, we provide a comprehensive ROM estimation of a recently discovered *Allosaurus fragilis* (HS0387), based on three-dimensional manipulation of the forelimbs following laser scanning morphology models.

The ROM of the forelimb or especially the manus has been analysed in numerous theropod taxa, including basal theropods (*Megapnosaurus rhodesiensis* Galton 1971; *Herrerasaurus ischigualastensis* Sereno 1993; *Coelophysis bauri* Carpenter 2002; *Dilophosaurus wetherilli* Senter and Sullivan 2019), abelisaurids (*Carnotaurus sastrei* Senter and Parrish, 2006), allosauroids (*Allosaurus fragilis* Carpenter 2002; *Acrocanthosaurus atokensis* Senter and Robins 2005), the tyrannosauroids (*Tyrannosaurus rex* Carpenter 2002; *Australovenator wintonensis* White et al 2015; *Guanlong wucaii* Yu et al 2015), the ornithomimosaurians (*Deinocheirus mirificus* Osmólska and Roniewicz 1969; *Gallimimus sp.* and *Harpymimus okladnikovi* Kobayashi and Barsbold 2005; *Ornitholestes hermanni* Senter 2006a), an oviraptorosaurian (*Chirostenotes pergracilis* Senter and Parrish 2005) and the dromaeosaurids (*Bambiraptor feinbergi* Senter 2006b; *Deinonychus antirrhopus* Gishlick 2001; Carpenter 2002; Senter 2006b; troodontid Yu et al. 2022).

Carpenter (2002) illustrated the ROM estimates for some joints within the digits as well as the shoulder and elbow of several theropods, based on cartilage limits inferred from avian anatomy. Carpenter's analysis indicate that *Allosaurus'* arm could grasp medium-sized prey and pull it towards the body. The new specimen used herein (HS0387) exhibits palaeopathological asymmetry between the right and left forelimbs (Xing et al. 2024) (Figure 1), a condition whose implications for ROM of *Allosaurus* entire arms have not previously been explored. Here, we attempt to fill gaps in the published literature of *Allosaurus* by performing new estimates of the ROM and assessing the effect of paleopathology on ROM in the joints of forelimbs.

Motion orientation in extinct archosaurs can overlook the impact of soft tissue on joint ROM, leading to direct bone-to-bone contact at the joint. Cartilage affects limb length to some extent, and research has progressed on the functioning of joints with the addition of cartilage (Holliday et al. 2010; Hutson and Hutson 2012; Senter and Sullivan 2019). However, it is still not possible to accurately determine the degree to which cartilage morphology differs from the underlying skeleton. Moreover, there are significant morphological differences between cartilage epiphyses and hypophyses of different extant taxa (e.g. *Alligator mississippiensis* Hutson and Hutson 2012; *Struthio camelus* Holliday et al. 2010). As in the above studies (e.g. White et al 2015; Senter and Sullivan 2019; Yu et al. 2022), we still applied previous archosaur findings to reconstruct the ROM in forearm joints of *Allosaurus* by traditional bare-bones manipulations as the best method to determine its predatory role and to get further understanding of theropods evolutionary heritage. Absolute values determined this way are unlikely to map to *in vivo* ROM, but are useful as comparative data between skeletons, and as qualitative assessments of limb flexibility.

2 Material and methods

The *Allosaurus fragilis* specimen HS0387 was excavated from Dana Quarry in Ten Sleep, Wyoming, which is located in the Upper Jurassic Morrison Formation (Late Kimmeridgian-Early Tithonian). HS0387 is now in the collection of the Grandview Museum of Natural Science, Guangzhou, China. Xing et al. (2024) had demonstrated that the characteristics of HS0387 are consistent with the diagnosis of *Allosaurus fragilis* (Madsen 1976). The specimen is quite complete, with the forelimbs preserving the scapula, coracoid, humerus, radius and ulna, as well as the palm including the wrist bones on both sides. Only a few of the proximal articular surfaces of the phalanx are incomplete, as described in more detail below for ROM assessment. The high-quality surface shape of both forelimbs of *Allosaurus fragilis* specimen HS0387 was extracted using an Artec Space Spider scanner. of the scans were then digitally mounted for ROM evaluation in computer-aided design (CAD, 3ds MAX (2018) in this case).

Our joint ROM assessment primarily relies on the bare-bones method used in prior studies, in which the edges of manipulated three-dimensional (3D) articular surfaces delineate joint motion boundaries (Carpenter 2002; Senter and Robins 2005; White et al. 2015; Senter and Sullivan 2019; Yu et al. 2022). In order to implement the bare-bones method of ROM estimation, the edges of the articular surfaces need to be determined as accurately as possible based on abrupt changes in texture and/or topology. Furthermore, it must be considered that, at a given joint, the borders of the articular surfaces of the proximal and distal bones are the limits of their extension, respectively. In actual manipulation, the proximal bone at the joint is often fixed first, and then the articular surface of the distal bone is allowed to reach, but not exceed, the articular surface limit of the proximal bone to determine the ROM (Senter 2006a, 2006b; Senter and Parrish 2005, 2006; White et al. 2015; Senter and Sullivan 2019; Yu et al. 2022).

3 Results

Comprehensive descriptions of the forelimb elements for *Allosaurus* used in this investigation have previously been presented in detail and will not be repeated here (Gilmore 1920; Madsen 1976). Carpenter (2002) has taken it a step further by analysing the forelimb ROM based on two-dimensional sketches converted from photographs. In the following section, we present the first upgraded 3D ROM analysis of four biomechanical regions: the shoulder, elbow, wrist, and fingers.

3.1 Range of Motion

Shoulder joints

The glenoids of *Allosaurus* are oriented posteroventrally (Figure 1 A, B), but both scapulocoracoids show varying degrees of deformity due to prenatal lesions. The description and diagnosis of the palaeopathology of *Allosaurus fragilis* HS0387 has been previously reported in detail (Xing et al. 2024). The swollen right glenoid is more posteroventrally orientated than the

left, which has a pronounced effect on the assessment of shoulder ROM. However, the left and right glenoid still conform to the typical morphology of early theropods and would prevent the humerus from extending beyond the sub-horizontal level of the scapula (Senter 2006c; White et al. 2015). The humeral head is more extensive and bulbous (Figure 2 A-F) on the posterior than anterior suggesting that it has a greater degree of retraction than protraction (Senter and Robins 2005). In proximal view (Figure 1 C, D), the deltopectoral crest is subperpendicular to the rest of the left humerus, whereas the right humeral head develops more obtusely and wider. The failure to develop a markedly enlarged deltopectoral crest of *Allosaurus* reduces the possibility of forceful retraction of the entire forelimb beyond a sub-vertical position (Figure 1 E, F).

The humerus was posed for maximum extension (flexion) with the anterior (posterior) edge of the humeral head aligned with the coracoid (scapular) lip of the glenoid cavity at the shoulder joints. Manipulation of the shoulder joint revealed that the humerus of *Allosaurus fragilis* HS0387, similar to that of *Australovenator wintonensis* and *Dilophosaurus wetherilli* (Holliday et al. 2010; White et al. 2015; Senter and Sullivan 2019), fails to fit precisely into the glenoid, as was the case with extant archosaurs, probably as a result of the absence of the cap of articular cartilage (Mallison 2010a, 2010b; Senter and Sullivan 2019). The left humerus can be retracted to a position subparallel (3°) to the scapula, and extended to 81° to the scapula (Figure 2 A-C). Maximum extension of the right humerus (80°) is similar to the left humerus (Figure 2 D-F). However, the retraction (15°) is restricted by pathological swelling of the right glenoid. It clearly makes the uninfected left shoulder glenoid more reliable as an indicator for *Allosaurus* more broadly, so a measurement of 78° (Table 1) was used in recording the ROM of the HS0387 shoulder, rather than the 65° deviation from the right shoulder (Figure 2 A-F).

Assessment of the range of humeral adduction and abduction can be performed around the sagittal axis of the shoulder joint (Figure 2 G, H), with the lateral margin of the humeral head aligned with the lateral margin of the glenoid in maximal abduction and the medial margin in maximal adduction (Mallison 2010a, 2010b; Senter and Sullivan 2019). We conclude that the maximum abduction and adduction angles for the right and left shoulders of HS0387 are 47° and 45°, respectively. The difference between the two is not significant, and the mean value of 46° was taken as the final measurement (Table 1). The glenoid labrum and the lateral medial extension of the humeral head in theropod dinosaurs form a semicylindrical structure that restricts the humerus's long-axis rotation. Therefore, at the shoulder joint between the scapula and the olecranon, only the above ROM in the two directions of extension-flexion and adduction-abduction are considered.

Elbow joint

The distal end of humerus consists of smaller radial and ulna condyles separated by a distinct

intercondylar groove (Figure 1 G, H). This groove is more uniform and symmetrical on the ulnar and radial condyles of the left distal humerus, but is more broadly concave on the medial side of the radial condyle and narrower on the ulnar condyle of the right distal humerus (Gilmore 1920; Carpenter 2002). The smooth connection of the isolated ulna and radius at the elbow joint is roughly defined by the medial impression of the proximal end of ulna. This also allows the radius to have the ability to slide smoothly along the long axis distally and proximally during forearm motion. However, this does not accurately define the relative position between the bones of the antebrachium (White et al. 2015). The final definition of the two bones is dependent on the good anastomosis of the medial depression of the distal end of ulna with the lateral facet of the distal radius (Figure 1 I-L). The articular surfaces of the elbow joint involved in *Allosaurus fragilis* HS0387 are well defined on the distal end of the both humerus as well as on the proximal radius and ulna, which meets the conditions for use of the protocol used in the previous study (Senter 2005, 2006b; Senter and Robins 2005; Senter and Parrish 2006; White et al. 2015; Senter and Sullivan 2019).

For maximum flexion, the edge of the proximal end of the radius head is aligned with the proximal edge of the radial condyle on the anterior humerus. The flexion limit of the forearm is reached when the intercondylar groove of the humerus meets the lateral portion of the proximal humeral facet of the ulna, and retraction can be up to 72° and 71° at the right and left elbow joints (Figure 2 J, L), respectively. The proximal edge of the distal articular surface, which is situated on the posterior facet of the humerus, should line up with the proximal edge of the ulnar trochlear notch for maximum extension. The left and right forearms extend up to 146° and 137° (Figure 2 I, K), respectively. Although the difference in morphology between the two ulnas is negligible, the medial subvertical depression of the distal end of the right radius is deeper than that in the left radius (Figure 1 K, L), possibly influenced by the forward transmission of paleopathology at the right shoulder joint (Xing et al. 2024). This is reflected in the elbow joint and will cause the left forearm to extend more anterolaterally even in an unstressed relaxed state. Therefore, 74° at the left elbow joint was ultimately taken as the assessment ROM value (Table 1), rather than the lower 66° at the right elbow joint, which is influenced by the swollen right shoulder joint.

Wrist joint

As in most other theropods (Carpenter 2002; Senter and Robins 2005; Senter 2006a, 2006b; White et al. 2015; Senter and Sullivan 2019), the distal ends of the radius and ulna lack surfaces capable of supporting rolling opposed to each other, preventing both active supination and pronation. The skeletal configuration of the antebrachia is such that the palms face medially. The morphology of the radial carpal bones is important in determining the articular relationship with the wrist (White et al. 2015). However, the radiale of *Allosaurus fragilis* HS0387 is flattened proximally, with a weakly domed distal surface, and lacks a distinct facet that can well articulate with the distal

carpal 1. This structure is also present in *Coelophysis* wrist joint and is considered a feature of primitive tetanuran (Colbert 1989; White et al. 2015). Senter and Robins (2005) proposed that the presence of additional cartilaginous padding on the radius of *Acrocanthosaurus* further impedes accurate ROM analysis. It is likely that the enthesial cartilaginous cap also develops on the radiale of *Allosaurus*, and thus we cannot accurately determine the mobility of the *Allosaurus* wrist joints.

Digits joint

Metacarpals I-II of both manus were preserved in natural compaction, but fortunately did not undergo significant deformation (Figure 3). Metacarpal II has a depression at the posterior lower lateral corner conforming to the upper medial corner of metacarpal III. The metacarpals together form a divergent 'folded fan-like' palm structure of *Allosaurus* as in *Australovenator wintonensis* and *Dilophosaurus wetherilli* (Carpenter 2002; White et al. 2015; Senter and Sullivan 2019). In contrast to the forelimb joints described above, the articular surfaces of the bones of the hand are tightly fitted and well demarcated, greatly reducing the difficulty of assessing the range of motion of the joint. Typically, the phalanges and claws stops are terminated in both dorsal and medial directions, preventing further relative movement (Figure 4). Here, the same methodology as in other investigations was employed (Senter 2005, 2006a, 2006b; Senter and Parrish 2005; Senter and Robins 2005; White et al. 2015; Senter and Sullivan 2019; Yu et al. 2022), wherein phalanges were posed at the boundaries defined by their articular surfaces. The ROM of all phalanges are measured with 3ds MAX.

In both manus of specimen HS0387, the confirmation of the ROM was hardly ever hampered by unknown articular relationships. More fortunately, the articular surfaces are near complete overall. Even though a few elements have partially incomplete articular surfaces, with the upper or lower half missing to a low degree. However, it is still possible to estimate the ROM with the preserved portion and another symmetrical hand. In both the right and left digit I, the articular surfaces of the elements are well preserved. The distal end of metacarpal I is twisted inward, which causes phalanx I-1 to appear further away from the rest of the finger. The internal and external condyles of metacarpal I exhibit asymmetry in size and shape, and this also causes phalanx I-1 to lean away from the other digits and to rotate about its long axis during flexion and extension, similar to the plesiomorphic for Archosauria (Gauthier 1984). Specifically, the tip of claw I converges slightly towards the other fingers in flexion, with all fingers exhibiting a more regularly inwardly retracted appearance (Figure 3 C, D); and significantly away from the other fingers in extension (Figure 3 A, B). The dorsoventral flange on the articular surface of the metacarpal condyle acts as a bony stop (Figure 4). Corresponding measurements on the ROM were 40-18° of extension and 31-58° of flexion for the left finger I, whereas 43-16° of extension and 33-58° of flexion for the right finger I were observed (Fig. 4 A, B). For subsequent statistical studies, the average of the intact right and left fingers I were taken as the final ROM values of finger I for *Allosaurus fragilis*

HS0387 (Table 1).

In finger II, the proximal phalanx is capable of hyperextension (Figure 4 C, D), unlike the more straightened metacarpophalangeal I (Figure 4 A, C). Left finger II extended 25-22-12° and flexed 38-41-69° (Figure 4 C), whereas right finger II extended 18-24-12° and flexed 39-41-68° (Figure 4 D), and the dorsoventral flange on the articular surface of the metacarpal condyle again acts as a bony stop. The right manual phalanx II-1 was so compressed and deformed that the proximal articular surface was poorly preserved (Figure 4 D), so the ROM values in the left manus were used as the final measurements (Table 1). Similar processes were also taken in the right manual phalanx III-1, and in the left manual phalanx III-2 (Figure 4 E, F). In finger III, the proximal phalanx is further hyperextended than in finger II (Fig. 4 C-F). The left manual phalanx III-3 was used to restrict the extension as having incomplete articular surfaces in the upper part, but the lower part was in congruence with that at the right hand, and thus the manipulation of its upper part was based on its symmetry with that of the right hand (Figure 4 E). Extension of left finger III was 28-31-26-11° and flexion was 32-31-47-85° (Figure 4 E), whereas extension of right finger III was 27-26-25-12° and flexion was 33-30-45-85° (Figure 4 F). Considering the incomplete articular surfaces in the above, 60-62-72-97° were finally taken as the ROM measurements of the finger III for *Allosaurus fragilis* HS0387 (Table 1). Flexion range of all phalanges of the finger III of *Allosaurus fragilis* HS0387 exceeded 30°, which has been significantly reduced from 45° of the early theropod *Dilophosaurus wetherilli* (Senter and Sullivan 2019). This also consistent with the tendency for manus extension to decrease with divergence in theropods (Senter 2006a,2006b; White et al. 2015; Senter and Sullivan 2019; Yu et al. 2022).

3.2 Forelimb Function in *Allosaurus fragilis*

Carpenter (2002) summarised the wide range of hypotheses about the usages of the forelimbs, suggesting that most of the statements were unsubstantiated ‘arm-waving’ and not as extensive as analyses of the hindlimb. Senter (2006b) stepped further and presented a table of hypotheses about the motions that a theropod could have performed with their forelimbs, accompanied by a series of predictions for a range of morphological characters and minimum ROM. As implemented in Senter and Sullivan (2019), we again refrain from belaboring the table, but endorse it as a convenient template for assessing forelimb function in theropods.

The morphology and ROM in the forelimbs of *Allosaurus fragilis* are inconsistent with some of the functional hypotheses that are also thought to be falsified in *Dilophosaurus wetherilli* (Senter 2006b; Senter and Sullivan 2019). Examples include scratch-digging or hook-and-pull digging, which requires long enough forelimbs and fingers that could be flexed to reach the palms, a condition that neither of the above fulfils. In contrast, the slender fingers of the more derived theropods, such as *Chirostenotes pergracilis*, are more suitable for hook-and-pull digging similar

to the foraging behaviour of extant anteaters or pangolins (Senter and Parrish 2005; Senter 2006b). The morphology and ROM of *Allosaurus fragilis* HS0387 forelimbs are consistent with the following functional hypotheses (Senter 2006b): palms, fingers, and/or claws assume important role for grasping and maintaining objects; grasping and maintaining small-diameter, lightweight objects with one hand; hooking or seizing objects located within accessible range of motion of the forelimbs on the ventral surface of the chest; scratching with the fingers on parts of the body; bringing an object up to the mouth; or holding the object tightly in place on the thoracic region; and swinging the arms in a parasagittal arc along both sides of the rib cage to display.

4 Discussion

4.1 Comparison with Carpenter' Results

We are not the first to investigate the range of motion of the forelimb of *Allosaurus fragilis*. Carpenter (2002) compared and examined the motion of the entire forelimbs of five theropods, including *Allosaurus fragilis*, based on those of birds and crocodiles. Our results on the forelimb mobility are similar in some aspects to those reported by Carpenter (2002) on the basis of casts and real bone forelimb specimens (USNM 4734 Gilmore, 1920), but also differ from them in others. Methodologically, Carpenter used stands, clips and 'sticky' wax to support the bones in the correct anatomical position, assuming that the maximum motion of the joints was at the limit of the inferred cartilage that once covered the joint. The materials used by Carpenter (2002) were based on photographs or line drawings of fossils (overlapping masking of finger III affects the ROM measurements), incomparable to the accuracy of the 3D model of the entire forelimb used in this paper.

Carpenter (2002) illustrated that the humerus ROM of *Allosaurus fragilis* was between a subparallel but no more than perpendicular orientation to the scapula, which matches with our results (Figure 2 A-F). However, the arc of motion of the shoulder joint in the anterior was approximately 21°, which is much smaller than the 78° we measured at the left scapula without pathological deformity (Figure 2 C). Elbow flexion in both of these conclusions was restricted, with the forearm in full flexion passing over the vertical position of the humerus and forming an acute angle of about 70° with the humerus in both cases (Figure 2 J, L). Our results for the ROM in the fingers of *Allosaurus fragilis* are similar to those illustrated by Carpenter (2002), but we estimated a larger range of flexion of phalanx II-1 than his illustration (Figure 4). In recent years, the methods used to estimate ROM have been based on physical or more often 3D scans of the bones (White et al. 2015; Senter and Sullivan 2019; Yu et al. 2022). We suggest that the reason for the discrepancy between Carpenter's (2002) results and ours mainly stems from the methodology and the observation views in the final illustrations.

4.2 The Influence of Palaeopathology

Allosaurus is one of the most frequently found theropods from the Upper Jurassic Morrison Formation, and its osteological aberrations are among the most frequently reported afflictions in palaeopathology (e.g. Madsen 1976; Rothschild 1988; Hanna 2002; Foth et al. 2015; Xing et al. 2024). The results of our analyses of *Allosaurus fragilis* forelimbs indicate that palaeopathology should be included when reconstructing the specific parts ROM of an extinct individual. In HS0387, the pectoral girdle and dorsal vertebrae are preserved with a large number of palaeopathological peculiarities suggested that this prehistoric predator suffered from spondyloarthropathy during its lifetime (Xing et al. 2024). In the right scapulocoracoid of HS0387, a swollen pathological condition at the glenoid has caused considerable remodelling of the entire right forearm (Figure 1). These conditions not only imparted the morphogenetic asymmetry of the right forelimb, but further resulted in the series of ROM differences that we have inferred here.

HS0387 is a subadult with pathological deformities that not only cause the right glenoid to be more laterally orientated, but also the two openings to be different in size (Figure 1 A, B). In addition, the asymmetry between the forelimbs is transmitted forward to the humeral head, the lateral ulnar condyle of the humerus as well as to the medial articular surface of the distal end of ulnar (Figure 1 C, D, G, H, K, L). It may be to accommodate a change in the way force is generated by the proximal forelimb. Our ROM estimation yielded a neutral position of the right humerus closer to the torso with a smaller ROM than the left humerus. More specifically, the pathological condition directly affected *Allosaurus fragilis* HS0387 right shoulder ROM and passed forward to influence the ROM of the right elbow joint.

The variety of pathologies of the subadult *Allosaurus fragilis* HS0387 was interpreted by Xing et al. (2024) as possible trauma, infection, spondyloarthropathy, or tumour-related, none of which inherently would have caused the outright death of an animal. The deformation of the articular surfaces and different ROM of the scapula and its distal child elements suggests that the asymmetry due to the lesions at the right shoulder joint was transmitted forward to the right elbow and wrist joints. The subadult died with all of its injuries cured, suggesting that the pathology occurred long before the skeleton was stereotyped into a dead condition. Therefore, we hypothesise that the pathology of the right shoulder joint in this living animal occurred prior to rapid ontogeny to meet our finding that the development of the joints of the sub-elements was affected. This inference is supported by the degree of spinal fusion due to spondylolisthesis described in Xing et al. (2024).

From the perspective of individual skeletal developmental deformities, the infection in the right shoulder joint of this living animal persisted for a long period of time. This could have resulted not only in reduced mobility of the right forelimb, but also in a change to the way the forelimb

was incorporated. Foth et al. (2015) suggested that *Allosaurus* had a relatively active predatory life. Further, this effect of these injuries on the long-term diminution of the hunting ability of HS0387 could have been amplified in the scenario of active predation. Therefore, our study on the pathobiomechanics of the right forelimb of HS0387 also supports the conclusion proposed by Xing et al. (2024) that the cause of the ultimate death of the individual could be a shortage of food due to a change in the predation pattern.

4.3 Comparison with Other Dinosaurs

Many studies have been performed on the ROM of manus in theropods, including the early theropods (Carpenter 2002; Senter and Parrish 2005; Senter and Sullivan 2019), allosauroids (Carpenter 2002; Senter and Parrish 2005; Yu et al. 2015), tyrannosauroids (Carpenter 2002; Senter and Parrish 2005; White et al. 2015), oviraptorosaurian (Kobayashi and Barsbold 2005; Senter and Parrish 2005; Senter 2006b), and dromaeosaurids (Senter and Parrish 2005; Senter 2006a; Yu et al. 2022) (Table 2). Carpenter (2002) first analysed the limiting positions of each joint of the forelimbs of five theropods, which were photographed and converted into sketches, and the hyperextension and flexion values based on the line drawings were used in subsequent studies of the forelimb ROM in theropods (Senter and Parrish 2005; White et al. 2015; Yu et al. 2022).

In most theropods, the range of forelimb extension-flexion and adduction-abduction was determined primarily by glenoid. For example, in *Allosaurus* both glenoid labria are equally well developed (Figure 1 A, B), whereas they are asymmetrically developed in cf. *Coelurus* and *Deinonychus*, and less developed *Tyrannosaurus* (Carpenter 2002). The anterior and posterior glenoid labria of *Allosaurus* was prominent, so extension-flexion was more restricted than adduction-abduction. In these latter theropods, the medial labria was lower than the lateral one, and the glenoid surface was sloped between them. This position placed the scapular glenoid ventrally, thus preventing the humerus from flexing past the subhorizontal level of the scapula blade. Quadrupeds had a more laterally orientated glenoid and used retraction of the humerus around the vertical axis to propel themselves (Baier and Gatesy 2013). Bipeds, however, had no need for support in their forelimbs, allowing the glenoid to be reoriented to alter the ROM of humerus (Senter 2006c). The altered humeral motion in Dinosauria was predominantly parasagittal, rather than transverse, favouring the grasping of prey below the chest. Further extension of glenoid in the avian evolutionary branch elevated the humerus laterally and could have some functional importance as, for example, in relation to the display of forelimb feathers in birds (Zelenitsky et al, 2012; Senter and Sullivan 2019).

Our estimation of the range of shoulder flexion and extension (78°) of *Allosaurus fragilis* is similar to that of *Dilophosaurus wetherilli* (85°) (Senter and Sullivan 2019). However, in

coelurosaurs, the humerus swings in a much more varied arc, such as the lower *Tyrannosaurus rex* (65°), but larger *Bambiraptor feinbergi* (103°) and *Deinonychus antirrhopus* (105°) (Carpenter 2002; Senter 2006b). Likewise, the range of elbow flexion and extension estimated from bare bone manipulation of *Allosaurus fragilis* (74°) is similar to that of *Acrocanthosaurus atokensis* (78°), but larger than that of the elbow of early theropod *Dilophosaurus wetherilli* (48°) and *Tyrannosaurus rex* (45°) (Carpenter 2002; Senter and Robins 2005; Senter and Sullivan 2019). Moreover, some of later Coelurosauria *Ornitholestes hermanni*, *Bambiraptor feinbergi*, and *Deinonychus antirrhopus* had elbow flexions of about 90° (Senter and Parrish 2005; Senter 2006a, 2006b). Our new findings of *Allosaurus* supported the inference of Senter and Sullivan (2019) that the limited shoulder and elbow ROM of early theropods appears to have been a plesiomorphic condition in Dinosauria, whereas Coelurosauria and Ceratopsia was a derived condition.

The medial orientation of *Allosaurus fragilis* palms is the plesiomorphic condition for Dinosauria (Gishlick 2001; Carpenter 2002; Senter and Robins 2005; Senter 2006b; Senter and Sullivan 2019), because the lack of a suitable articular surface for the distal antebrachium prevents the radius from actively rotating into a pronated position. As for the manual joints, the ROM varied widely from the most proximal metacarpophalangeal joint (Figure 6). Extension ranged from *Bambiraptor feinbergi* metacarpophalangeal joint III -4° to *Dilophosaurus wetherilli* metacarpophalangeal joint II 105° (Senter 2006b; Senter and Sullivan 2019), while flexion ranged from *Australovenator wintonensis* metacarpophalangeal joint I 10° to *Harpymimus okladnikovi* 70° (Kobayashi and Barsbold 2005; White et al. 2015). As for the interphalangeal joints, particularly finger II, their flexion ranged from 31° to 75° (Senter and Robins 2005; White et al. 2015), but low-extension conditions were present in almost all ornithomimosaurians and pennaraptorans (Senter and Parrish 2005; Senter 2006b). The range of flexion of the ungual joints was mostly >35°, but the range of extension ranged from *Australovenator wintonensis* >35°, *Acrocanthosaurus atokensis* and ornithomimosaurs in permanent flexion to pennaraptorans <10° (Senter and Robins 2005; White et al. 2015; Yu et al. 2022).

Our observations show that all metacarpophalangeal joints in early-diverging theropods showed a larger range of extension than flexion (Table 2), such as *Dilophosaurus wetherilli*, allosauroids and tyrannosauroids, but the opposite was true in *Coelophysis bauri* and maniraptoriforms (Figure 6). Moreover, within the same digit in tetanurans, there was an overall tendency for the range of flexion from proximal to distal phalanges to increase. This pattern became more stable in Maniraptoriformes, except for the apparently different finger II in *Chirostenotes pergracilis* and finger III in *Deinonychus antirrhopus* (Figure 6 B). Interestingly, the overall ROM trend was more analogous to the range of flexion (Figure 6 B, C), except that *Acrocanthosaurus atokensis* was variable (Senter and Robins 2005). It also suggests that the fingers of the bipedal theropods were dominated by flexion rather than extension, and function more to support the manus in achieving

grasping motions. In summary, the primitive condition of theropoda exhibits a considerable degree of hand hyperextension, as in coelophysoids, allosauroids and tyrannosauroids (White et al. 2015), whereas manual hyperextension is significantly reduced in divergent evolutionary clades, such as in ornithomimosaurians, oviraptorosaurians and dromaeosaurids (Figure 6). Overall, there is an overall increasing trend in manual flexion in these theropods, accompanied by a more pronounced decreasing trend in extension from early-diverging theropods to maniraptoriforms (Senter and Parrish 2005; White et al. 2015; Yu et al. 2015; Yu et al. 2022). The trend of early theropods manus hyperextension is further supported by the significantly higher manual extension capability in HS0387.

4.4 Functional and Behavioral Inferences

Various hypotheses have been suggested by previous authors about the forelimb function of theropods (Carpenter 2002; Senter and Parrish 2005; Senter 2006b; White et al. 2015; Senter and Sullivan 2019). The posterior humeral head is larger and more bulbous than the anterior, indicating a higher degree of retraction than protraction (Figure 2 A-F). The lack of a noticeably larger deltopectoral crest reduces the likelihood that the entire forelimb could be forcefully retracted (Senter and Robins 2005). These indicate that the shoulder and elbow joints are capable of supporting limited and weak manoeuvres. The distal end of antebrachium of HS0387 lacks the articular surfaces that could support the relative roll of the ulna and radius, and the flat articular surfaces of the carpal elements only permit the palm to face medially but prevent further active supination and pronation. In fact, both palms were oriented opposite each other towards the body's midline, and the animal was unable to move its forelimbs so that the palms faced the ground (Senter and Parrish 2005). As well, elbow flexion together with shoulder adduction allows the palms to be brought further medially. This allows *Allosaurus fragilis* to bring their hands together to grasp and maintain a grip on an object, suggesting that the palms and/or palmar surfaces of fingers are the dominant organs of prehension.

The forearm ROM comparisons of *Allosaurus fragilis* with other theropod groups (Carpenter 2002; Senter and Parrish 2005; Senter 2006b; White et al. 2015; Senter and Sullivan 2019; Yu et al. 2022), especially *Dilophosaurus wetherilli* (Senter and Sullivan 2019), enhances understanding of the functional role played by the forelimb in predation. As with other bipedal theropods, the medially-facing palms and hyperextension of digits in *Allosaurus* were not suitable for body support. The fingers allowed a large degree of passive motion, possibly to prevent fingers dislocation caused by violent struggles by prey， as in *Dilophosaurus wetherilli* (Senter and Sullivan 2019). Based on the morphology and ROM of manus in *Allosaurus fragilis* HS0387, it has been surmised that it could be used in direct prey activities such as grasping, ripping and racking, or indirect activities such as hooking, digging and clamping. Carpenter (2002) argued that the overall range of motion of the relatively long and robust forelimbs of *Allosaurus fragilis* (USNM 4734) suggests that its arms

could grasp medium-sized prey and pull it toward its body. This also coincides with our analyses on the function of the forelimbs of HS0387. There is a large range of finger hyperextension in tyrannosauroid *Australovenator wintonensis* (White et al. 2015), which possibly possesse unique manual functions beneficial to predation. In dromaeosaurids, the manus are conditioned to have a large range of flexion but a limited range of extension, and predation is mainly achieved by means of the oral or a sickle-like claw on the toe II whereas the manus are more likely to be used only for supplementary grasping (Ostrom 1969; Manning et al 2009; White et al 2015). In *Allosaurus fragilis*, the ability to hyperextend is slightly lower than in *Australovenator wintonensis*, but the range of flexion is still similarly large. This situation suggests that, in contrast to the later-derived forms, *Allosaurus* were more likely to use their manus to prey rather than simply grasp. In general, decreased manual extension in theropods is likely correlated with altered manus functions.

However, it is impossible to ignore that the forelimb ROM imposes important constraints on the prey size and predatory behaviour of *Allosaurus*, such as proportionally shorter forelimbs and restrictedly mobilized shoulders. In hunting, the manus only seized smaller prey located within the forelimbs ROM near the chest and neck. However, the sharp-toothed muzzle of *Allosaurus* was able to reach farther than the manus, which is more advantageous when making first contact with larger prey. Previous studies of the predatory behaviour of both *Dilophosaurus wetherilli* and *Acrocanthosaurus atokensis* made similar inferences about their resemblance to the forelimbs ROM of *Allosaurus fragilis* (Senter and Robins 2005; Senter and Sullivan 2019). There were also theropods with a wider shoulder ROM, such as the Dromaeosauridae, that were able to catch prey farther to body side with their forelimbs (Senter 2006b). The forelimb joints and the shape and length proportions of humerus heads of *Allosaurus fragilis* are similar to those of basal theropods (Sereno 1993; Senter and Robins 2005; Senter and Sullivan 2019), such as *Herrerasaurus ischigualastensis*, *Dilophosaurus wetherilli*, and *Acrocanthosaurus atokensis*, and therefore forelimbs predation restriction is regarded as a plesiomorphy condition of Theropoda.

5 Conclusions

We examined the forelimb of Upper Jurassic Morrison Formation *Allosaurus fragilis* HS0387, analysing the range of motion of the shoulder, elbow, wrist and fingers. The humerus could be retracted to a position subparallel to the scapula and extended no more than a subvertical position. Elbow flexion may be at an acute angle to the humerus. The lack of a rolling radial-ulnar joint prevents active pronation and rotation with the palm facing medially. Digit I is separated from the other fingers in hyperextension, and the ability to flex is greater than the ability to extend. We also discuss the effect of palaeopathology on the inferred ROM of *Allosaurus fragilis*, where the right forelimb with damage present is not as mobile as the left forelimb at the shoulder and elbow joints. Only prolonged pathology at the right shoulder joint could have had a transmissive effect on the development of the child skeleton at its elbow joint. Coupled with the fact that his injuries

were consistent with a number of conditions that were not directly fatal, we suggest that disease occurs well before immature HS0387 exhibits the skeletal development that was seen at the time of death. ROM analyses of manus show a relatively large range of extension and flexion in this animal, which is consistent with trends in the finger hyperextension and extension abilities of early-diverging theropods. Functions reflected in forelimb morphology and ROM are consistent with the hypothetical prediction of a two-handed grasping, maintaining an object on the chest, manually hooking or seizing the object, and holding the prey on the chest or under the neck of predator.

Acknowledgements

Acknowledgements are extended to Grandview Museum of Nature Science (GMNS), Guangzhou, China, for its valuable contribution to the collection of specimen HS0387. We would like to express our gratitude to Institute of Vertebrate Paleontology and Paleoanthropology for providing the Artec Space Spider scanning equipment and Donghao Wang of the China University of Geosciences (Beijing) for his invaluable scanning assistance.

Disclosure statement

No potential conflicts of interest were reported by the author(s).

Funding

This research was funded by the "Deep-time Digital Earth" Science and Technology Leading Talents Team Funds for the Central Universities for the Frontiers Science Center for Deep-time Digital Earth, China University of Geosciences (Beijing) (Fundamental Research Funds for the Central Universities; grant number: 2652023001), the 111 project (B20011), Fundamental Research Funds for Central Universities (265QZ201903).

Reference

Baier DB, Gatesy SM. 2013. Three-dimensional skeletal kinematics of the shoulder girdle and forelimb in walking *Alligator*. Journal of Anatomy. 223:462-473. https://doi.org/10.1111/joa.12102.

Bates KT, Benson RB, Falkingham PL. 2012. A computational analysis of locomotor anatomy and body mass evolution in Allosauroidea (Dinosauria: Theropoda). Paleobiology. 38(3):486-507. doi:10.1666/10004.1.

Carpenter K. 2002. Forelimb biomechanics of nonavian theropod dinosaurs in predation. Senckenbergiana lethaea. 82(1):59-75. doi:10.1007/BF03043773.

Chure DJ, Loewen MA. 2020. Cranial anatomy of *Allosaurus jimmadseni*, a new species from the lower part of the Morrison Formation (Upper Jurassic) of Western North America. PeerJ. 8:e7803. Doi:10.7717/peerj.7803.

Colbert EH. 1989. The Triassic dinosaur *Coelophysis*. Museum of Northern Arizona Bulletin. 57: 1-160.

Foth C, Evers SW, Pabst B, Mateus O, Flisch A, Patthey M, Rauhut OWM. 2015. New insights into the lifestyle of Allosaurus (Dinosauria: Theropoda) based on another specimen with multiple pathologies. PeerJ 3:e940. doi:10.7717/peerj.940.

Galton PM. 1971. Manus movements of the coelurosaurian dinosaur *Syntarsus* and opposability of the theropod hallux. Arnoldia. 5(15):1-8.

Gauthier JA. 1984. A cladistic analysis of the higher systematic categories of the Diapsida. University of California, Berkeley.

Gishlick AD. 2001. The function of the manus and forelimb of *Deinonychus antirrhopus* and its importance for the origin of avian flight. In: Gauthier J, Gall LF, editors. New Perspectives on the Origin and Early Evolution of Birds. New Haven (CT): Yale Peabody Museum; p. 301-318.

Gilmore CW. 1920. Osteology of the carnivorous Dinosauria in the United State National museum: with special reference to the genera *Antrodemus* (*Allosaurus*) and *Ceratosaurus*. US Government printing office. 110(110):1-159. doi:10.5479/si.03629236.110.i.

Holliday CM, Ridgely RC, Sedlmayr JC, Witmer LM. 2010. Cartilaginous epiphyses in extant archosaurs and their implications for reconstructing limb function in dinosaurs. PLoS ONE. 5(9):e13120. doi:10.1371/journal.pone.0013120.

Hutson JD, Hutson KN. 2012. A test of the validity of range of motion studies of fossil archosaur elbow mobility using repeated-measures analysis and the extant phylogenetic bracket. Journal of Experimental Biology. 215(12):2030-8. doi:10.1242/jeb.069567.

Kobayashi K, Barsbold R. 2005. Anatomy of *Harpymimus okladnikovi* Barsbold and Perle 1984 (Dinosauria; Theropoda) of Mongolia. In: Carpenter K, editor. The Carnivorous Dinosaurs. Bloomington (IL): Indiana University Press. p. 97-126.

Madsen JHJ. 1976. *Allosaurus fragilis*: a revised osteology. Utah Geological and Mining Survey Bulletin. 109:3-163.

Mallison H. 2010a. The digital Plateosaurus I: body mass, mass distribution, and posture assessed using CAD and CAE on a digitally mounted complete skeleton. Palaeontologia electronica. 13(2): 1-26.
Mallison H. 2010b. The Digital Plateosaurus II: An Assessment of the Range of Motion of the Limbs and Vertebral Column and of Previous Reconstructions using a Digital Skeletal Mount. Acta Palaeontologica Polonica. 55(3): 433-458. doi:10.4202/app.2009.0075.
Manning PL, Margetts L, Johnson MR, Withers PJ, Sellers WI, Falkingham PL, Mummery PM, Barrett PM, Raymont DR. 2009. Biomechanics of dromaeosaurid dinosaur claws: application of X-ray microtomography, nanoindentation, and finite element analysis. The Anatomical Record: Advances in Integrative Anatomy and Evolutionary Biology. 292(9):1397-1405. doi:10.1002/ar.20986.
Marsh OC. 1877. Notice of new dinosaurian reptiles from the Jurassic formation. American Journal of Science. 14(84):514-516. doi:10.2475/ajs.s3-14.84.514.
Osmólska H, Roniewicz E. 1969. Deinocheiridae, a new family of theropod dinosaurs. Palaeontologica Polonica. 21:5-19.
Rayfield EJ. 2005. Aspects of comparative cranial mechanics in the theropod dinosaurs *Coelophysis*, *Allosaurus* and *Tyrannosaurus*. Zoological Journal of the Linnean Society. 144(3):309-16. doi:10.1111/j.1096-3642.2005.00176.x.
Senter P. 2006a. Forelimb function in *Ornitholestes hermanni* Osborn (Dinosauria, Theropoda). Palaeontology. 49:1029-1034. doi:10.1111/j.1475-4983.2006.00585.x.
Senter P. 2006b. Comparison of forelimb function between *Deinonychus* and *Bambiraptor* (Theropoda: Dromaeosauridae). Journal of Vertebrate Paleontology. 26(4):897-906. doi:10.1671/0272-4634(2006)26[897:COFFBD]2.0.CO;2.
Senter P. 2006c. Scapular orientation in theropods and basal birds, and the origin of flapping flight. Acta Palaeontologica Polonica. 51(2): 305-315.
Senter P, Parrish JM. 2005. Functional analysis of the hands of the theropod dinosaur *Chirostenotes pergracilis*: evidence for an unusual paleoecological role. PaleoBios. 25(2):9-19.
Senter P, Parrish JM. 2006. Forelimb function in the theropod dinosaur *Carnotaurus sastrei*, and its behavioral implications. PaleoBios. 26(3):7-17.
Senter P, Robins JH. 2005. Range of motion in the forelimb of the theropod dinosaur *Acrocanthosaurus atokensis*, and implications for predatory behaviour. Journal of Zoology. 266(3):307-318. doi:10.1017/S0952836905006989.
Senter P, Sullivan C. 2019. Forelimbs of the theropod dinosaur *Dilophosaurus wetherilli*: range of motion, influence of paleopathology and soft tissues, and description of a distal carpal bone. Palaeontologia Electronica. 5:1-19. doi:10.26879/900.
Sereno PC. 1993. The pectoral girdle and forelimb of the basal theropod *Herrerasaurus ischigualastensis*. Journal of Vertebrate Paleontology. 13(4):425-450. doi:10.1080/02724634.1994.10011524.
Smith DK. 1998. A morphometric analysis of *Allosaurus*. Journal of Vertebrate Paleontology. 18(1):126-142. doi:10.1080/02724634.1998.10011039.
Snively E, Cotton JR, Ridgely R, Witmer LM. 2013. Multibody dynamics model of head and neck function in *Allosaurus* (Dinosauria, Theropoda). Palaeontologia Electronica. 16:1-29. doi:10.26879/338.
White MA, Bell PR, Cook AG, Barnes DG, Tischler TR, Bassam BJ, Elliott DA, Carrier D. 2015. Forearm range of motion in *Australovenator wintonensis* (Theropoda, Megaraptoridae). PLoS one. 10(9): e0137709. doi 10.1371/journal.pone.0137709.
Xing L, Rothschild BM, Du C, Wang D, Wen K, Su J. 2024. New palaeopathology cases of *Allosaurus fragilis* (Dinosauria: Theropoda). Historical Biology. 36(1):203-8. doi:10.1080/08912963.2022.2155817.
Yu D, Pei R, Yin YL, Zhou CF. 2022. The morphology and function of the manual digits of a troodontid from the Yixian Formation of western Liaoning, China. Historical Biology. 36(1):183-92. doi:10.1080/08912963.2022.2155149.
Yu YL, Sullivan C, Xu X. 2015. Three-dimensional modeling of the manual digits of the theropod dinosaur *Guanlong*, with a preliminary functional analysis. Acta Palaeontologica Sinica. 54(2):165-173.
Zelenitsky DK, Therrien F, Erickson GM, DeBuhr CL, Kobayashi Y, Eberth DA, Hadfield F. 2012. Feathered non-avian dinosaurs from North America provide insight into wing origins. Science. 388:510-514. https://doi.org/10.1126/science.1225376.

610 **Figures**

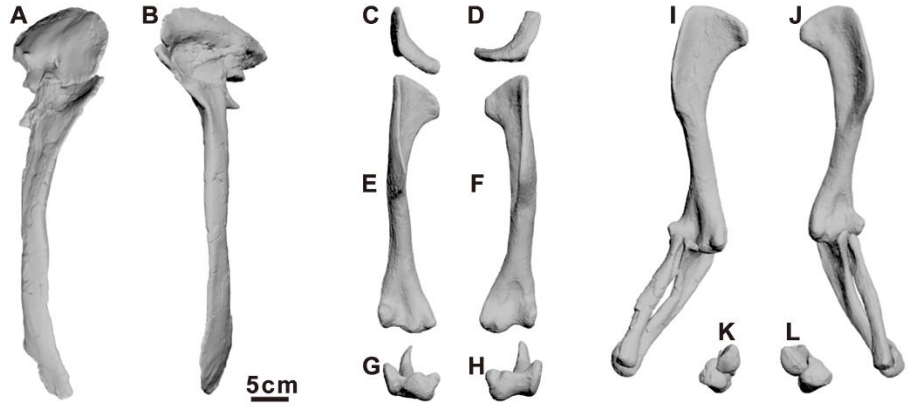

611
612 Figure 1. The articular surfaces of scapulocoracoid, humerus, radius, and ulna of *Allosaurus*
613 *fragilis* HS0387. Left (A) and right (B) scapulocoracoid in lateral view; right and left humerus in
614 proximal (C, D), cranial (E, F) and distal (G, H) views; right and left humerus and antebrachium
615 extended in medial (I, J) and distal (K, L) views.
616

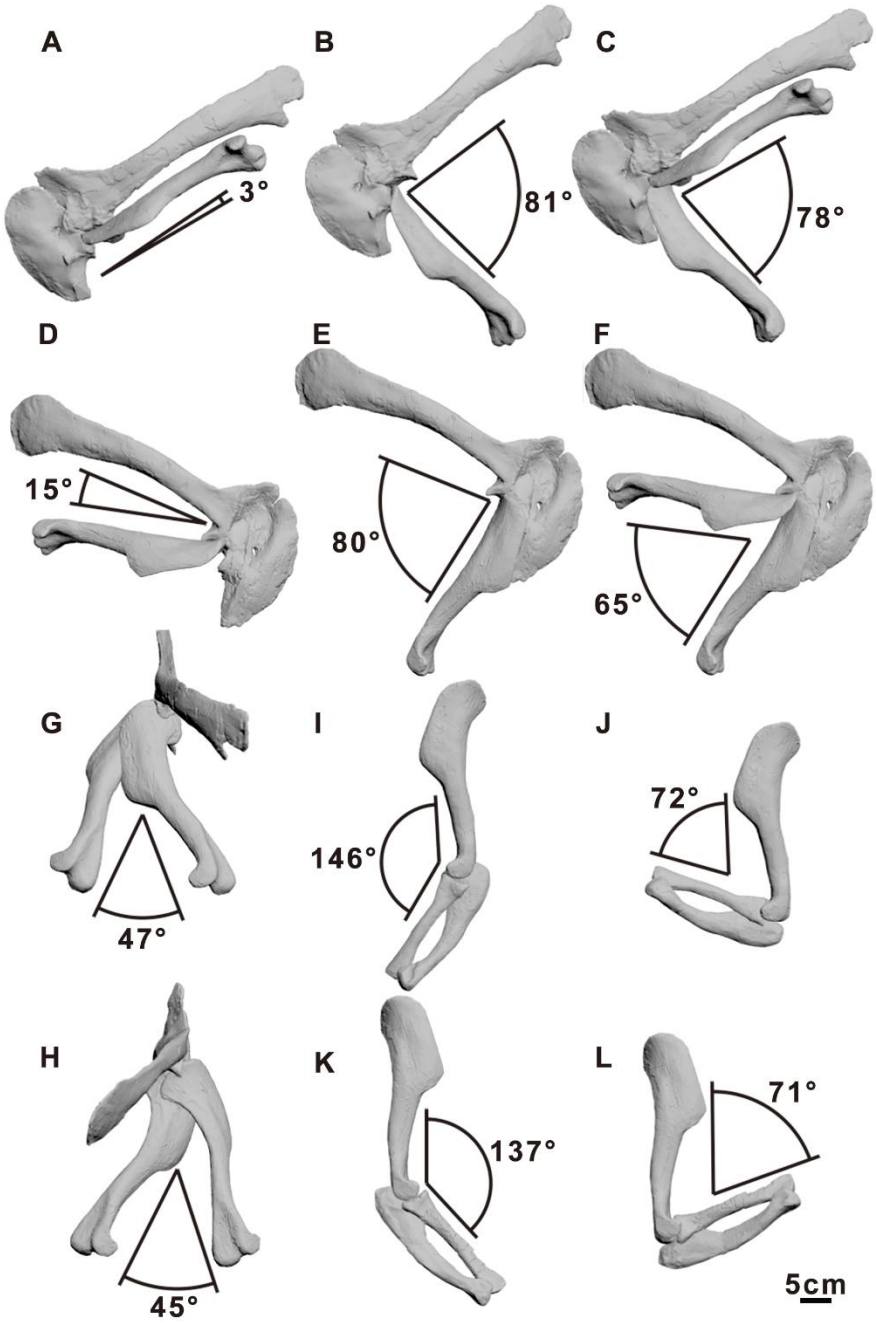

Figure 2. The range of motion in the forelimbs of *Allosaurus fragilis* HS0387. A-F, left and right scapulocoracoid and humerus flexed (A, D), extended (B, E) and both (C, F) in lateral view. Left (G) and right (H) scapulocoracoid and humerus adducted and abduced in dorsal view. I-L, left and right humerus and antebrachium flexed (I, K) and extended (J, L) in lateral view.

622

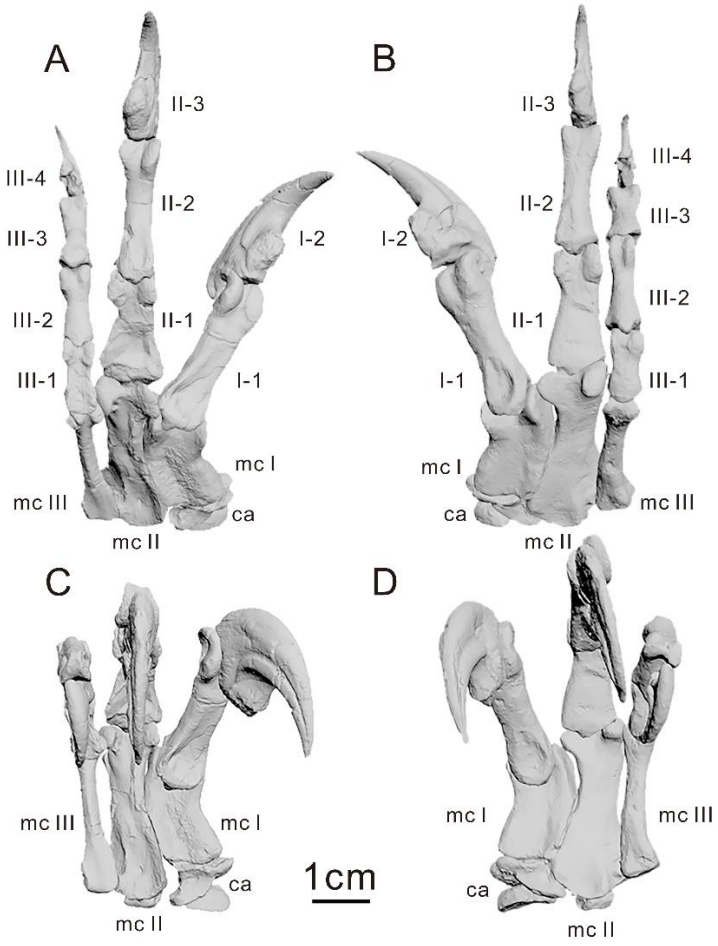

623

624 Figure 3. Two digital mounting manus of *Allosaurus fragilis* HS0387, palmar view. Right and left
625 straight (A, C) and flexed (B, D) digits. Abbreviations: I-1–I-2, the phalanges of the manual digit
626 I; II-1–II-3, the phalanges of the manual digit II; III-1–III-4, the phalanges of the manual digit III;
627 mcI–mcIII, the metacarpals I and III; ca, carpals.

628

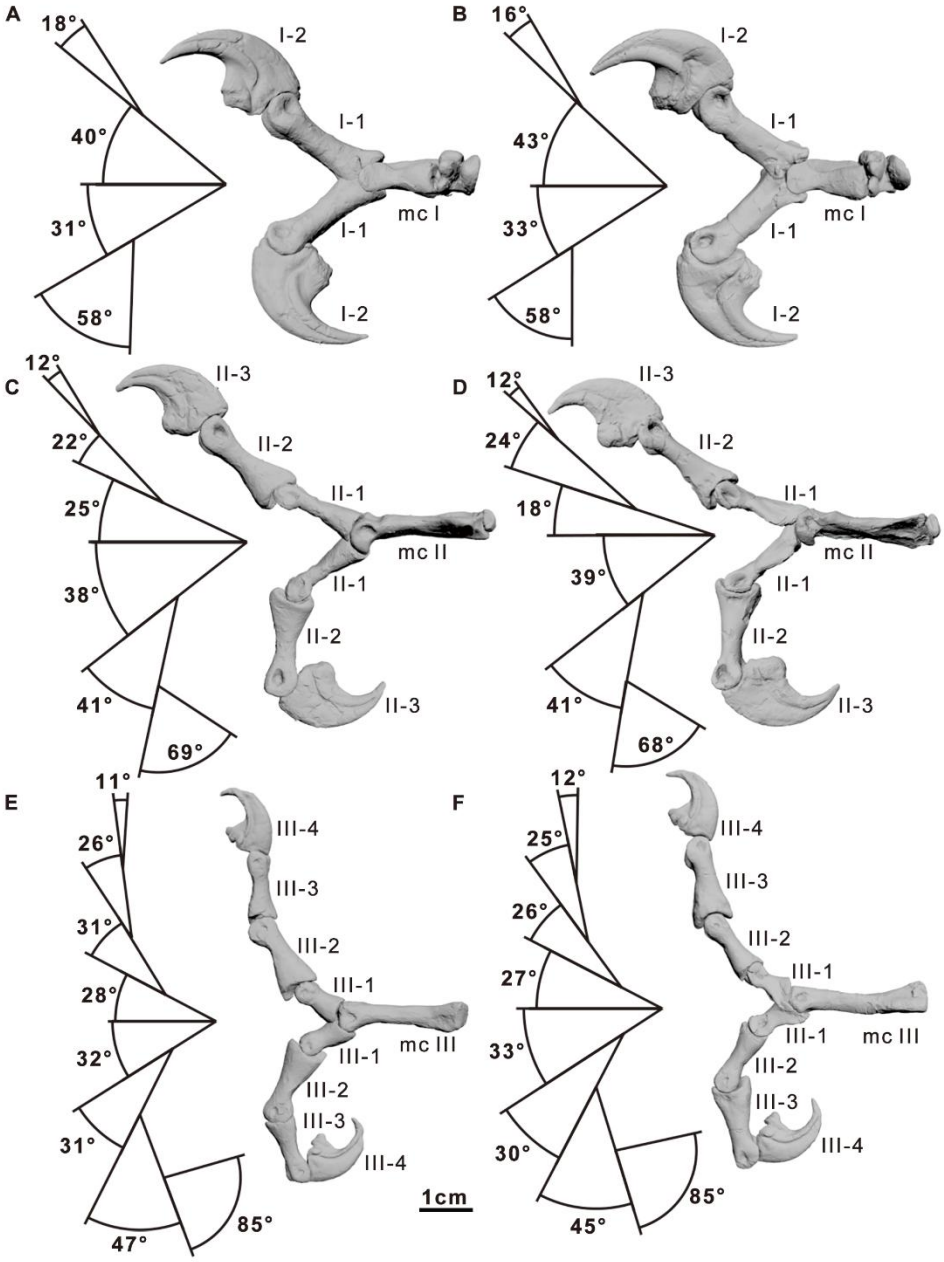

Figure 4. The range of motion in the fingers of *Allosaurus fragilis* HS0387. A-F, left and right digit I (A, B), digit II (C, D) and digit III (E, F) extended (upper) and flexed (lower) in lateral view. Abbreviations: I-1–I-2, the phalanges of the manual digit I; II-1–II-3, the phalanges of the manual digit II; III-1–III-4, the phalanges of the manual digit III; mcI–mcIII, the metacarpals I and III.

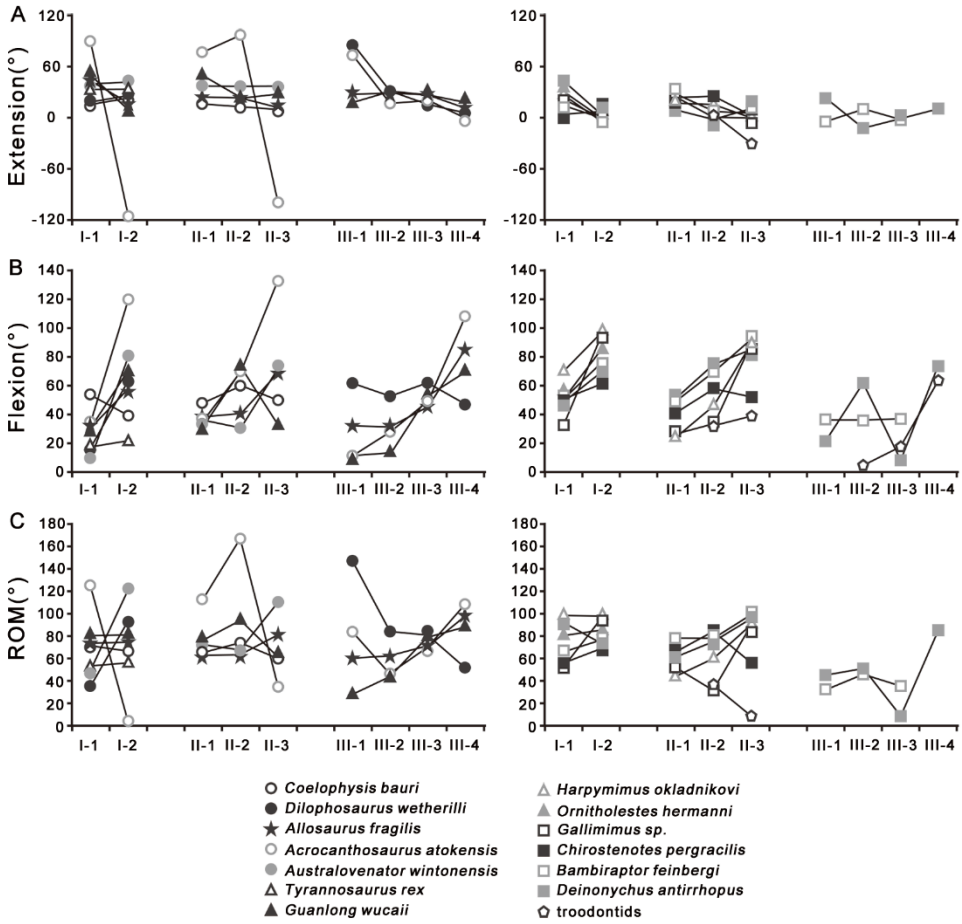

Figure 4. Ranges of extension (A), flexion (B) and ROM (C) within the same digit in theropods.

Tables

Table 1. Ranges of motion values of manual phalanges of *Allosaurus fragilis* HS0387 and USNM 4734 (the latter specimen date are from Carpenter 2002).

Specimens		Humerus	Forearm	I-1	I-2	II-1	II-2	II-3	III-1	III-2	III-3	III-4
HS0387	Extension	81	146	40	18	25	22	12	28	31	26	11
Left	Flexion	3	72	31	58	38	41	69	32	31	47	85
	ROM	78	74	71	76	63	63	81	60	62	73	96
Right	Extension	80	137	43	16	18	24	12	27	26	25	12
	Flexion	15	71	33	58	39	41	68	33	30	45	85
	ROM	65	66	76	74	57	65	80	60	56	70	97
Final ROM		**78**	**74**	**74**	**75**	**63**	**64**	**81**	**60**	**62**	**72**	**97**
USNM 4734	Extension	74	136	55	15	20	10	0	?	?	?	8
	Flexion	53	63	19	62	18	63	58	?	?	?	87
	ROM	21	73	74	77	38	73	58	?	?	?	95

Table 2. ROM values of various theropods in comparison with *Allosaurus fragilis* (Carpenter 2002; Senter and Parrish 2005; Senter and Robins 2005; Kobayashi and Barsbold 2005; Senter 2006a, 2006b; White et al 2015; Yu et al 2015; Senter and Sullivan 2019; Yu et al. 2022).

Dinosaur taxon		Humerus	Forearm	I-1	I-2	II-1	II-2	II-3	III-1	III-2	III-3	III-4
Coelophysis bauri	E	?	?	18	26	17	13	10	?	?	?	?
	F	?	?	54	40	48	60	50	?	?	?	?
	R	?	?	**72**	**66**	**65**	**73**	**60**	?	?	?	?
Dilophosaurus wetherilli	E	?	?	19	28	105	?	18	85	31	18	5
	F	?	?	16	65	21	?	27	62	53	62	47
	R	**85**	**48**	**35**	**93**	**126**	?	**45**	**147**	**84**	**80**	**52**
Allosaurus fragilis	E	81	146	42	17	25	23	12	28	31	26	12
	F	3	72	32	58	38	41	69	32	31	46	85
	R	**78**	**74**	**74**	**75**	**63**	**64**	**81**	**60**	**62**	**72**	**97**
Acrocanthosaurus atokensis	E	?	144	90	-116	77	97	-98	73	18	20	0
	F	?	66	35	119	36	70	133	11	28	50	108
	R	?	**78**	**125**	**3**	**113**	**167**	**35**	**84**	**46**	**70**	**108**
Australovenator wintonensis	E	?	?	40	42	38	37	37	?	?	?	50
	F	?	?	10	80	36	31	73	?	?	?	62
	R	?	?	**50**	**122**	**72**	**68**	**110**	?	?	?	**112**
Tyrannosaurus rex	E	?	?	35	34	?	?	?	?	?	?	?
	F	?	?	18	22	?	?	?	?	?	?	?
	R	**65**	**45**	**53**	**56**	?	?	?	?	?	?	?
Guanlong wucaii	E	?	?	49	10	46	22	28	17	30	26	18
	F	?	?	31	71	31	72	33	11	14	53	70
	R	?	?	**80**	**81**	**77**	**94**	**61**	**28**	**44**	**79**	**88**
Harpymimus okladnikovi	E	?	?	28	0	19	14	0	?	?	?	?
	F	?	?	70	97	25	46	90	?	?	?	?
	R	?	?	**98**	**97**	**44**	**60**	**90**	?	?	?	?
Ornitholestes hermanni	E	?	58	29	0	?	?	17	?	?	?	?
	F	?	37	52	85	?	?	100	?	?	?	?
	R	?	**95**	**81**	**85**	?	?	**117**	?	?	?	?
Gallimimus sp.	E	?	?	20	0	25	0	0	?	?	?	?
	F	?	?	33	96	27	33	90	?	?	?	?
	R	?	?	**53**	**96**	**52**	**33**	**90**	?	?	?	?
Chirostenotes pergracilis	E	?	?	5	7	24	25/16	4	?	?	?	?
	F	?	?	51	62	41	58/60	52	?	?	?	?
	R	?	?	**56**	**69**	**65**	**83/76**	**56**	?	?	?	?
Bambiraptor feinbergi	E	?	127,136	15	0	28	7	6	-4	10	-2	?
	F	?	59,55	51	76	50	70	92	36	36	37	?
	R	**103**	**68,81**	**66**	**76**	**78**	**77**	**98**	**32**	**46**	**35**	?
Deinonychus antirrhopus	E	?	150	43	4	10	0	11	23	-11	0	11
	F	?	51	49	70	51	75	85	22	62	9	74
	R	**105**	**99**	**92**	**74**	**61**	**75**	**96**	**45**	**51**	**9**	**85**
troodontids	E	?	?	?	?	?	4	-30	?	0	?	0
	F	?	?	?	~71	?	32	39	?	5	~18	64
	R	?	?	?	?	?	**36**	**9**	?	5	?	**64**

Abbreviations: E, extension; F, flexion; R, range of motion. '?' represents the measurements are unavailable, '~' represents the estimated value.